NOTICE

The quality of this microform is heavily dependent upon the quality of the original thesis submitted for microfilming. Every effort has been made to ensure the highest quality of reproduction possible.

If pages are missing, contact the university which granted the degree.

Some pages may have indistinct print especially if the original pages were typed with a poor typewriter ribbon or if the university sent us an inferior photocopy.

Previously copyrighted materials (journal articles, published tests, etc.) are not filmed.

Reproduction in full or in part of this microform is governed by the Canadian Copyright Act, R.S.C. 1970, c. C-30.

AVIS

La qualité de cette microforme dépend grandement de la qualité de la thèse soumise au microfilmage. Nous avons tout fait pour assurer une qualité supérieure de reproduction.

S'il manque des pages, veuillez communiquer avec l'université qui a conféré le grade.

La qualité d'impression de certaines pages peut laisser à désirer, surtout si les pages originales ont été dactylographiées à l'aide d'un ruban usé ou si l'université nous a fait parvenir une photocopie de qualité inférieure.

Les documents qui font déjà l'objet d'un droit d'auteur (articles de revue, tests publiés, etc.) ne sont pas microfilmés.

La reproduction, même partielle, de cette microforme est soumise à la Loi canadienne sur le droit d'auteur, SRC 1970, c. C-30.

Canada

Classification of Digitized Curves Represented by Signatures and Fourier Descriptors

Hussein S. El Buaeshi

A Project

in

The Department

of

Computer Science

Presented in Partial Fulfillment of the Requirements
for the Degree of Master of Science at
Concordia University
Montréal, Québec, Canada

June 1988

ISBN 0-315-44808-3

ABSTRACT

Classification of Digitized Curves Represented by Signatures and Fourier Descriptors

Hussein S. El Buaeshi

This is to study a classification of discrete contours via signatures. Two algorithms to compute the signature have been developed. In the first algorithm a multidimensional sorting is used. The second algorithm is based on simple geometrical considerations. Two types of signatures are considered —the length signature and the area signature. Statistical features based on Fourier descriptors are derived from the signatures. In the classification stage the k-NN algorithm is used where k and the size of the feature vector have been experimentally chosen. The algorithms have been tested on 840 handwritten, totally unconstrained characters from Suen's data base. The recognition success rates of 91% and 93% were achieved for the length and area signature respectively.

Acknowledgements

I would like to express my best thanks to my supervisor Dr. Adam Krzyzak, for his support and encouragement. The successful results achieved in this report are due to the discussion and advice given by him. I also wish to thank Dr. C. Y. Suen, for his support.

Contents

Notations x

1 Introduction 1

2 Feature Extraction 4

2.1 Curve Signature 4

2.2 Fourier Descriptors 5

3 Signature Computation 9

3.1 Algorithm 1 10

3.1.1 Pseudo-code of algorithm 1 10

3.1.2 The analysis of algorithm 1 11

3.2 Algorithm 2 12

3.2.1 Pseudo-code of algorithm 2 12

3.3 Algorithm 3 14

3.3.1 Pseudo-code of algorithm 3 14

3.3.2 The analysis of algorithm 3 16

3.4 Changes to algorithm 3 19

4 Classification 20

4.1 Differentiation Scheme 32

5 Conclusion 39

Bibliography 40

A Signature expansion 43

B Detailed Pseudo-code of algorithm 1 46

C Proof of Lemma 2.1 49

List of Tables

4.1 Classification rates for different sizes of feature vector (FD's (amplitudes) of the length signature) and different number of k-nearest neighbors. 25

4.2 Classification rates for different sizes of feature vector (FD's (phase-angles) of the length signature) and different number of k-nearest neighbors. 25

4.3 The confusion matrix for classification using the FD's (phase-angles) of the length signature. 26

4.4 The confusion matrix for classification using the FD's (phase-angles) of the area signature. 27

4.5 The confusion matrix for classification using FD's (amplitudes) of the length signature. 28

4.6 The confusion matrix for classification using FD's (amplitudes) of the area signature. 29

4.7 The differentiating inequalities for the length signature. 34

4.8 The differentiating inequalities for the area signature. 34

4.9 The confusion matrix for the classification scheme using the length signature. 36

4.10 The confusion matrix for the classification scheme using the area signature. 37

List of Figures

1.1 The basic components of the implemented character recognition system. 3

2.1 The continuous line is a signature value at link Q of the polygon. 8

2.2 The filled area is another signature value at link Q of the polygon. 8

3.1 The translation and rotation of the coordinate system. 12

3.2 Finding the length $\overline{P_f P_w}$ to the left of the current link $\overline{P_i P_j}$, where $P_f \neq P_1$, (step 2.) 16

3.3 Finding the length $\overline{P_e P_m}$ to the left of the current link $\overline{P_i P_j}$, where $P_e \neq P_n$, (step 2.) 17

3.4 Finding the length $\overline{P_1 P_n}$ to the left of the current link $\overline{P_i P_j}$, where $P_e = P_n$ and $P_f = P_1$, (step 3.) 17

3.5 Finding the length $\overline{P_t P_r}$ to the left of the current link $\overline{P_i P_j}$, where $t < r$, $|t - r| = 1$, (step 4.) 18

3.6 Finding the length $\overline{P_t P_o}$ to the left of the current link $\overline{P_i P_j}$, where $t < r$, $|t - r| \neq 1$, (step 4.) 18

3.7 Finding the length $\overline{P_r P_s}$ to the left of the current link $\overline{P_i P_j}$, where $t < r$, $|t - r| \neq 1$, (step 4.) 19

4.1 Some of the numerals used in the experiment. . . . 21
4.2 The length signatures of some numerals. 23
4.3 The area signatures of some numerals. 24
4.4 Numeral 8 misclassified as 9, because the lower part is small compared to the upper part of the numeral . . 31
4.5 Fat numeral 8 misclassified as 0 32
4.6 The four equal intervals of the signature. 33
4.7 The classification scheme for the length signature . . 38
4.8 The classification scheme for the area signature . . . 38

A.1 The signature function. 43

Notations

Symbol	Explanation
i,j,l,r,t,w,z,m,o,e	vertex indices or loop index.
P_1	the first vertex of the polygon.
P_n	the last vertex of the polygon.
P_f	the first vertex to the left of the current link.
P_e	the last vertex to the left of the current link.
V_i	the i^{th} vertex.
$\lambda(\cdot)$	array contains the vertices to the left of the current link.
+	the left side of the link.
-	the right side of the link.
Γ	the unit polygon.
$S(t)$	the signature at point t.
$S^*(t)$, $S^{*'}(t)$	the normalized signature.
x, u	x coordinate of a vertex.
y, v	y coordinate of a vertex.
$\cup$	union of two sets.
n	number of vertices of a polygon.
d, s	the slope of a tangent line.
$N_I[j]$	array contains the good indices of the vertices and their reflections.
L	the total length of the polygon.
Q	the current link.

Symbol	Explanation
M	number of subsets.
g	loop index.
m_k	the slope of the ray k.
J_{qi}	the i^{th} index of a vertex in the subset q.
t	the arc length.
a_m	the m^{th} Fourier coefficient.
α_m	the m^{th} phase angle.
$Re\ a_m$	the real part of the Fourier coefficient a_m.
$Im\ a_m$	the imaginary part of the Fourier coefficient a_m.
A_m, A'_m	the m^{th} amplitude of the Fourier coeficient.
$\{A_m, \alpha_m\}_0^n$	the Fourier Descriptors.
signature(·).length	the length of the numeral on and to the left of the current link.
signature(·).area	the area of the numeral to the left of the current link.
Multi-algorithm	the multidimensions sorting algorithm (Length signature).
Simple-algorithm	the geometrical consideration alogrithm (Length signature).
Area-algorithm	the algorithm computes the area (Area signature).
Δl	the length of the link.
$k(j)$	the number of the subset within which j lies.
c_j	the length or area to the left of the current link.
I_A	the indicator function of set $A = [l_{i-1}, l_i]$.

Chapter 1

Introduction

In many pattern recognition applications and digital image processing the shape of a simply connected object is represented by its outer contour. Many shape recognition techniques deal with the boundary of the entire object, the silhouette, the intensity profile or range map. These include such methods as Fourier descriptors of the object boundary [2,6,7,9,12,13,17,18,20], moments of the silhouette [3], and circular autoregressive models [8]. Among different techniques, Fourier descriptors and curve signatures are distinguished by the invariance to the standard shape transformations such as scaling, rotation and translation. Some functions of Fourier descriptors are also invariant to mirror reflections and changes in the starting point [9,17]. In this project the shape recognition problem using Fourier descriptors (FD's) derived from the curve signatures will be studied. This approach combines the simplicity of curve signatures with invariance of Fourier descriptors. The length signature proposed by O'Rourke [13] is used here and the area signature is also introduced. The latter is shown to be more robust with respect to shape distortion. Efficient algorithms for computation of curve signatures have been proposed and implemented. In shape classification features

based on Fourier descriptors have also been used. Fourier descriptors derived from the signature are characterized by invariance to affine transformations and changes in the starting point. Several versions of Fourier descriptors have been studied and compared. The shape representation methods proposed in this project have been tested in unconstrained handwritten numerals. Basic components of the implemented recognition system are shown in Figure 1.1.

The feature extraction module consists of two sub-modules: a signature module and a Fourier descriptors module. In the signature module the algorithm based on the geometrical considerations has been used to compute the length/area signature of the numeral. The Fourier descriptors module computes the FD's of the numerals from their signatures. The classification module is divided into two sub-modules as follows:

1. k-NN sub-module to find the k-nearest neighbor using branch and bound algorithm [4].

2. signature verification sub-module to separate distinct numerals with similar FD's.

In sub-module 1, FD's are used alone. In sub-module 2, classification is based on the signature.

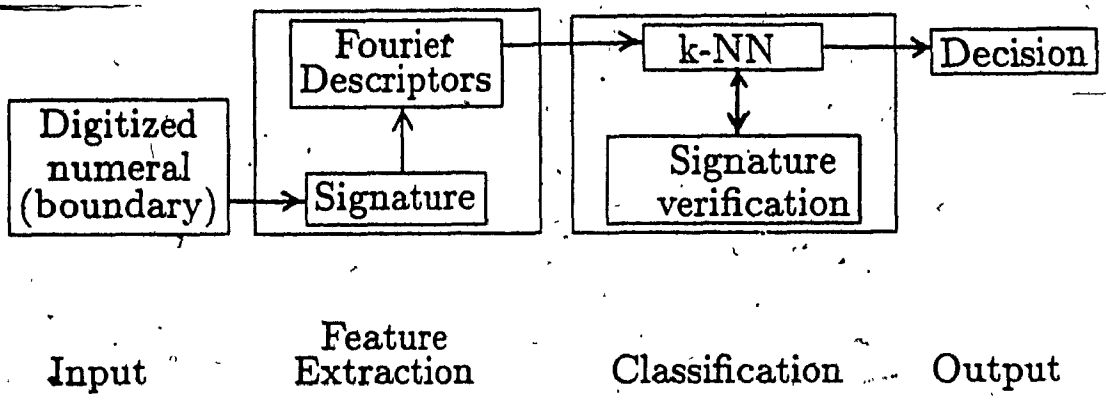

Figure 1.1: The basic components of the implemented character recognition system.

Chapter 2

Feature Extraction

The most popular feature extraction techniques used in shape recognition are: Fourier descriptors [7,17,20], boundary line encoding [12], polygonal approximation and directional and curvature feature extraction (see [19] for review). Here and in the following sections, feature extraction methods based on the signature and Fourier descriptors will be presented.

2.1 Curve Signature

O'Rourke defined a signature of a plane curve [14]: Let Γ be a continuous, directed curve in the Euclidean plane, parameterized by its arc length t. The signature S(t) of Γ is the function which associates with each point t of Γ the length of Γ which is on or to the left of a tangent line at point t —Figure 2.1. The alternative version of the signature is defined as an area to the left of a tangent line instead of the length to the left —Figure 2.2. The following formula is used to calculate the area of the polygonal figure with vertices $V_1 = (x_1, y_1), \ldots, V_n = (x_n, y_n)$,

$$area = \frac{1}{2} \left| \sum_{i=1}^{n} x_i (y_{i+1} - y_{i-1}) \right| \tag{2.1}$$

where subscripts are reduced modulo n and $y_0 = 0$.

The main advantages of curve signature are its simplicity (the histogram represents the signature of a polygon) and its invariance to shifts and rotations (so long as the starting point is maintained). The main weakness of the signature is that it does not uniquely identify the curve that it is derived from, except for rectilinear curves [14]. For instance, all convex curves of unit length are mapped on the constant signature at one or zero depending on the orientation. Nevertheless, the curve signature is a valuable tool in shape recognition as will be shown in the following sections.

In this project we consider the normalized signatures obtained by dividing the value of the signature at point t by the total length of the curve and by taking $S^*(t) = S(Lt)$, where L is the length of Γ $t \in [0, 1]$.

2.2 Fourier Descriptors

Fourier descriptors of plane curve were first introduced by Cosgriff [1] and were subsequently used by a number of researchers [2,7,9,12,13,17,18,20]. It is well known that similar shapes regardless of their size and location usually fall into the same cluster in the Fourier descriptor space using the Euclidean metric distance. New Fourier descriptors derived from the coefficients of a Fourier series that correspond to either the length or the area signature are proposed here.

Only polygonal curves are considered. Assume that the curve Γ

has n vertices $V_0, \ldots, V_n = V_0$ and that the edge (V_{j-1}, V_j) has the length Δl. The Signature is a step function given by equation

$$S^*(t) = \sum_{j=1}^{n} c_j \, I_{A_j}(Lt) \tag{2.2}$$

where $A_j = [l_{j-1}, l_j]$, $l_j = \sum_{k=1}^{j} \Delta l_k$ and $I_A(\cdot)$ is the indicator function of a set A. Coefficients c_j denote either the length of Γ to the left of the edge (V_{j-1}, V_j) in case of the length signature or the area bounded by Γ to the left of the edge (V_{j-1}, V_j) in case of the area signature. Fourier coefficients of $S^*(t)$ are given by the following equation:

$$a_m = \frac{1}{m\pi} \sum_{j=1}^{n} c_j \exp\left(-i\left(\frac{m2\pi l_{j-1}}{L} - \frac{\pi}{2}\right)\right)\left(\exp -i\left(\frac{m2\pi \Delta l_j}{L}\right) - 1\right)$$

$$a_0 = \frac{1}{L} \sum_{j=1}^{n} c_j \Delta l_j$$

where i is equal to $\sqrt{-1}$. Coefficient a_m may be expressed in the magnitude-phase form as:

$$\begin{aligned} a_m &= A_m \exp(i\alpha_m) \\ &\text{where} \\ A_m &= (Re^2(a_m) + Im^2(a_m))^{\frac{1}{2}} \\ Re(a_m) &= \frac{1}{m\pi} \sum_{j=1}^{n} c_j \cos\left(\frac{m\pi}{L}(2l_{j-1} + \Delta l_j)\right) \sin\frac{m\pi}{L}\Delta l_j \\ Im(a_m) &= \frac{-1}{m\pi} \sum_{j=1}^{n} c_j \sin\left(\frac{m\pi}{L}(2l_{j-1} + \Delta l_j)\right) \sin\frac{m\pi}{L}\Delta l_j \\ \alpha_m &= \arctan\frac{Im(a_m)}{Re(a_m)} \end{aligned} \tag{2.3}$$

The Fourier descriptors are defined as $\{A_m, \alpha_m\}_{-n}^{n}$. It can easily be shown that A_m's are not only invariant to translations, rotations and

scaling (that follows from the definition of $S^*(t)$ and eq. (2.3)), but also to changes in the starting point (see Lemma 2.1). On the other hand rotations affect the phase angles α_m's which can be used to distinguish between curves which are rotated versions of each other, for example characters 9 and 6. The problem of the choice of the number of FD's will be addressed in the following sections.

Lemma 2.1 *If Γ and Γ' are two curves which only differ in a sense that they are translation, rotations, or scaled version of each other or they only differ in the starting point by Δl_0 units of arc length then*

$$\begin{aligned} A_m &= A'_m \\ \alpha_m &= \alpha'_m + m\Delta t_0 \end{aligned}$$

For the proof see appendix C.

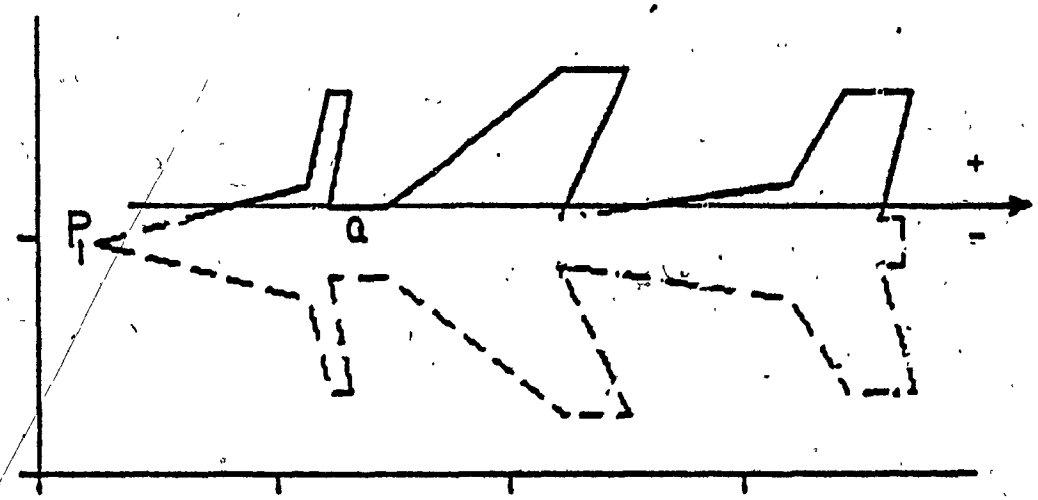

Figure 2.1: The continuous line is a signature value at link Q of the polygon.

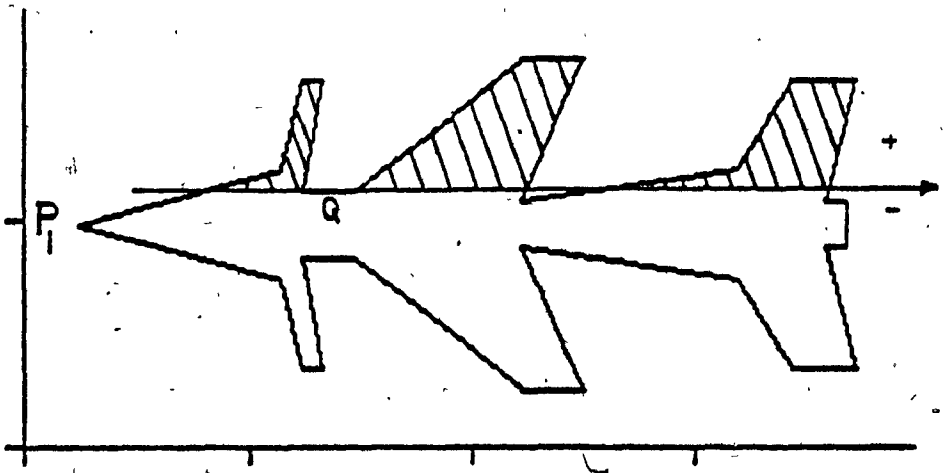

Figure 2.2: The filled area is another signature value at link Q of the polygon.

Chapter 3

Signature Computation

In this section, efficient algorithms which calculate the signature of a plane curve are presented. Algorithms 1 and 2 find the vertices to the left of the current link of the polygon. The first algorithm uses multidimensional sorting [5]. The second algorithm uses the simple geometrical properties of a polygon. Both algorithms use algorithm 3 to calculate the length or the area to the left of the current link of a polygon. These algorithms were written in Pascal language and executed on the MicroVax II workstation. Algorithm 2 is on average four times faster than algorithm 1. In the following sections, we will provide for each algorithm (1) algorithm description; (2) pseudo-code of the algorithm; and (3) for some algorithms a description of the algorithm steps— the analysis of the algorithm.

3.1 Algorithm 1

Description. The algorithm presented here uses the multidimensional sorting of [5]. It translates the coordinate system origin to a polygonal vertex $P_i, i = 1, \ldots, n$; reflects each vertex $P_j \neq P_i$, with respect to P_i yielding a vertex P_{n+j}, and sorts the vertices and their reflections circularly about P_i, the order within each ray about P_i being immaterial. In order to obtain the vertices to the left of the current origin P_i only the original vertices from the ray $\overline{P_iP_j}$ to the ray $\overline{P_iP_{j+n}}$ counterclockwise have to be identified.

3.1.1 Pseudo-code of algorithm 1

Input: $P_i = (x_i, y_i), 1 \leq i \leq n$.

Output: Signature(i).length/area, $1 \leq i \leq n$.

1. **For** $i = 1, \ldots, n$ **do** step 2 to 8.
2. **For** $j = 1, \ldots, n$ **do** $u_j = x_j - x_i$, $v_j = y_j - y_i$.
3. **For** $j = 1, \ldots, n$, **if** $(u_j, v_j) \neq (0, 0)$ call j "good".
4. **For** every good $j = 1, \ldots, n$ let $u_{j+n} = -u_j$, $v_{j+n} = -v_j$, and $s_{j+n} = \frac{v_j}{u_j}$, provided that $u_j \neq 0.0$.
5. The indices $\{j | j \text{ is good }\} \cup \{n + j | j \text{ is good}\}$ are to be sorted into subsets as follows
   (a) $\{j | u_j > 0; s_j - key\}$
   (b) $\{j | u_j = 0, v_j > 0\}$

(c) $\{j|u_j < 0; s_j \text{ —}key\}$

(d) $\{j|u_j = 0, v_j > 0\}$.

6. Find the vertices to the left of the current link $\overline{P_iP_j}$ by taking the original vertices going counterclockwise from the ray containing P_j to the ray containing its reflection P_{j+n}.

7. Sort the vertices to the left of the current link using the index as the key.

8. Signature(i).length = the length of the polygon to the left of the current link (use algorithm 3).
   Signature(i).area = the area bounded by the points on and to the left of the current link (use eq. 2.1 and algorithm 3).

3.1.2 The analysis of algorithm 1

Step 1 and 2 translate the coordinate system origin to a polygonal vertex P_i. Step 3 designates P_i as good if $P_i \neq P_j$. Step 4 reflects P_j with respect to P_i and finds the slope of $\overline{P_iP_j}$. Step 5 sorts the vertices and their reflection circularly about P_i. Steps 6, 7 and 8 are very clear.

3.2 Algorithm 2

Description. This algorithm is based on the simple geometrical properties of a polygon. It proceeds as follows. For each link of the polygon the coordinate system is rotated and translated so that the origin coincides with the starting vertex of the link. The x-axis is then aligned with the polygon link. The vertices (x, y) to the left of the link are the ones with $y \geq 0.0$ see Figure 3.1.

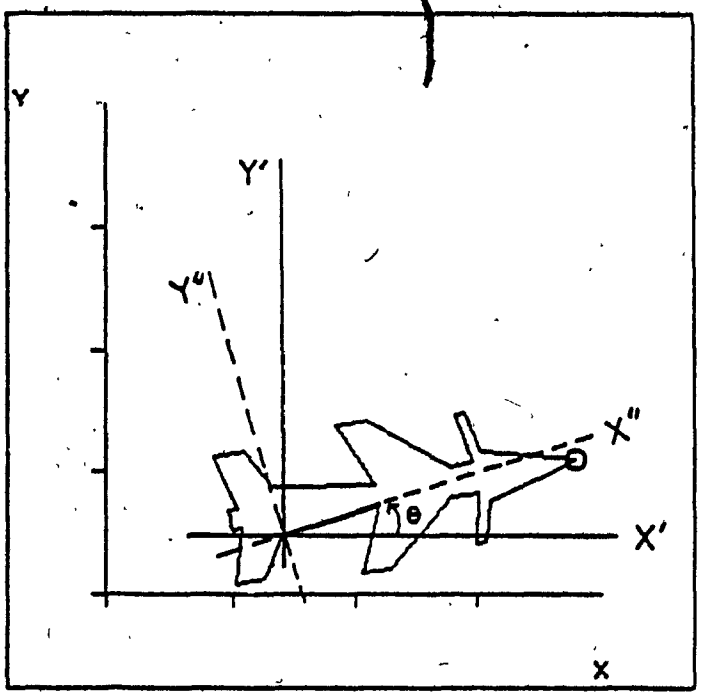

Figure 3.1: The translation and rotation of the coordinate system.

3.2.1 Pseudo-code of algorithm 2

Input: $P_i = (x_i, y_i), 1 \leq i \leq n.$

Output: Signature(i).length/area $1 \leq i \leq n.$

1. **For** $i = 1, \ldots, n$ **do** step 2 to 6.

2. Let $j = i + 1$.

3. Translate the coordinate system OXY by the vector $\overline{OP_i}$ to the coordinate system $P_iX'Y'$ as follows:

   - **For** $m = 1, \ldots, n$ **do**
     $x'_m = x_m - x_i, \quad y'_m = y_m - y_i.$

4. Rotate the coordinate system $P_iX'Y'$ through an angle θ about the origin P_i to the new coordinate system $P_iX''Y''$ as follows:

   - **For** $m = 1, \ldots, n$ **do**
     $x''_m = x_m \cos\theta + y'_i \sin\theta$
     $y''_m = -x'_m \sin\theta + y'_i \cos\theta.$

5. Find and sort all vertices $y''_m \geq 0.0$ to the left of the current link $\overline{P_iP_j}$ of the polygon using the index as a key.

6. Signature(i).length = the length of the curve to the left of the current link (compute the length using algorithm 3).
   Signature(i).area = the area bounded by the points on and to the left of the current link (use eq. 2.1 and algorithm 3.)

The steps of this algorithm are self explanatory.

3.3 Algorithm 3

This algorithm finds:

1. the intersection points between the ray containing the current link and the other links of the polygon.
2. the length of the line segments connecting the points on and to the left of the current link.

3.3.1 Pseudo-code of algorithm 3

Input: $\overline{P_iP_j}$, vertices to the left of the current link, number of vertices to the left of the current link.

Output: the total length of the line segments to the left of the current link.

Let $P_0 = P_n$, and $P_1 = P_{n+1}$.

1. Let P_f and P_e be the first and last points to the left of the current link.
2. **if** $f \neq 1$ **or** $e \neq n$ **then**
   begin
   - Let P_k be a point of the polygon such that $k = f - 1$.
   - Find the intersection between $\overline{P_iP_j}$ and $\overline{P_fP_k}$ say P_w.
   - Find the distance between P_f and P_w (which is the part of the link to the left of the current link.)
   - Let P_z be a point of the polygon such that $z = e + 1$.

- Find the intersection between $\overline{P_iP_j}$ and $\overline{P_eP_z}$ say P_m.
- Find the distance between P_e and P_m (which is the part of the link to the left of the current link.)

end.

3. **else** find the distance between P_1 and P_n.
4. Compute the length of the line segments connecting the vertices $P_f, \ldots, P_e$ as follows:
   - Let P_t and P_r be two consecutive vertices to the left of the current link such that $t < r$
   - **if** $t - r = 1$ **then** find the distance between P_t and P_r.
   - **if** $t - r \neq 1$ **then**

     begin
   - Find the intersection between $\overline{P_iP_j}$ and $\overline{P_tP_{t+1}}$ say P_o.
   - Find the distance between P_t and P_o (which is the part of the link to the left of the current link.)
   - Find the intersection between $\overline{P_iP_j}$ and $\overline{P_rP_{r-1}}$ say P_s.
   - Find the distance between P_r and P_s (which is the part of the link to the left of the current link.)

     end.
5. Total-length = the sum of the length of the line segments computed in either step 2 or step 3 and step 4.

3.3.2 The analysis of algorithm 3

Step 2 computes the length of the first and last line segment to the left of the current link, when both vertices P_1 and P_n do not occur together to the left of the current link—Figure 3.2 and Figure 3.3. The following figures explain the remaining steps of algorithm 3.

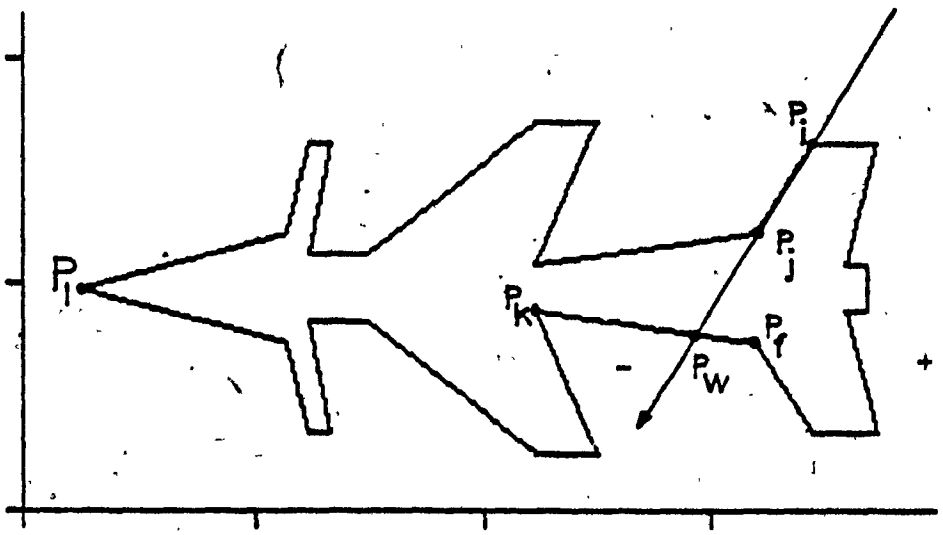

Figure 3.2: Finding the length $\overline{P_f P_w}$ to the left of the current link $\overline{P_i P_j}$, where $P_f \neq P_1$, (step 2.)

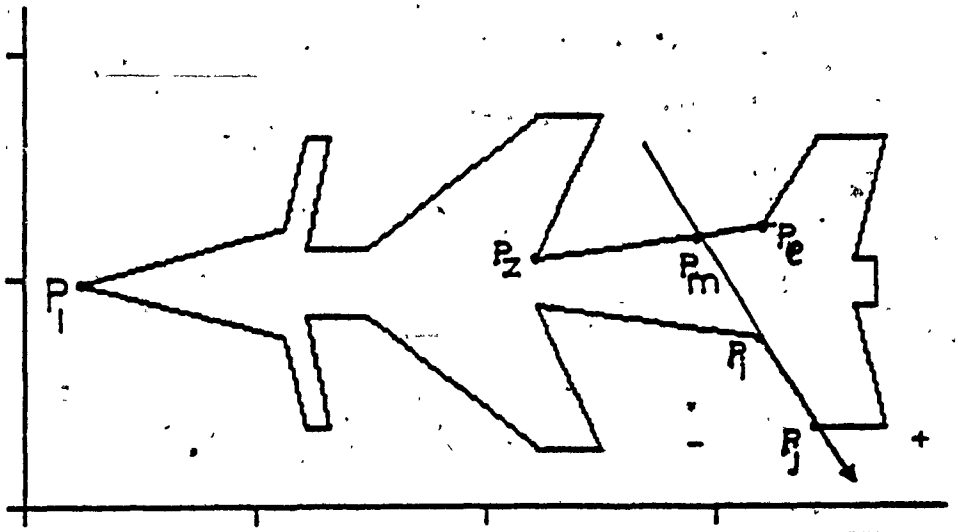

Figure 3.3: Finding the length $\overline{P_eP_m}$ to the left of the current link $\overline{P_iP_j}$, where $P_e \neq P_n$, (step 2.)

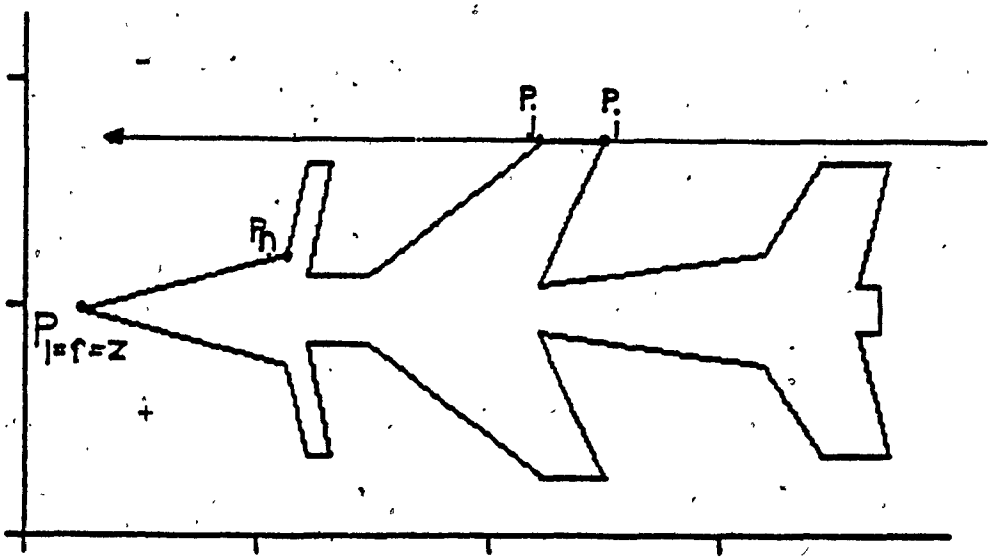

Figure 3.4: Finding the length $\overline{P_1P_n}$ to the left of the current link $\overline{P_iP_j}$, where $P_e = P_n$ and $P_f = P_1$, (step 3.)

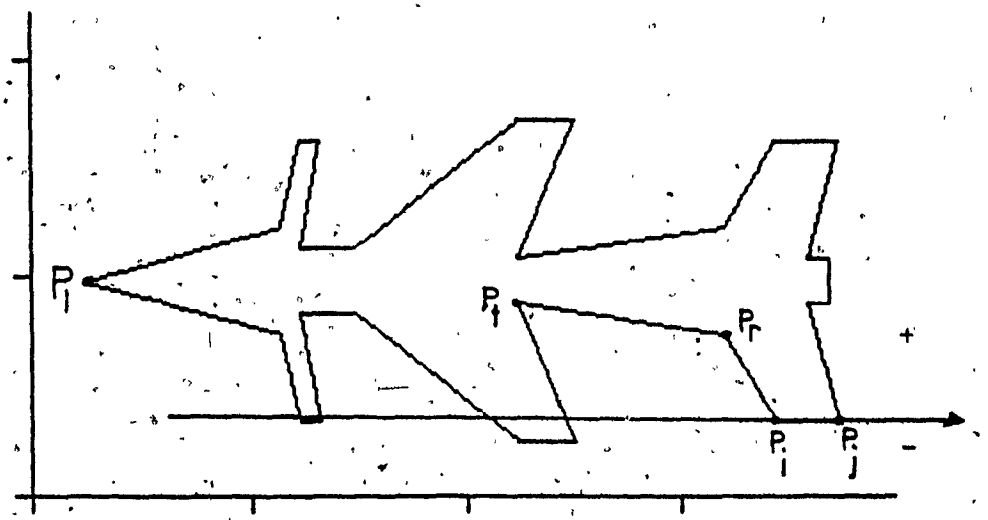

Figure 3.5: Finding the length $\overline{P_tP_r}$ to the left of the current link $\overline{P_iP_j}$, where $t < r$, $|t - r| = 1$, (step 4.)

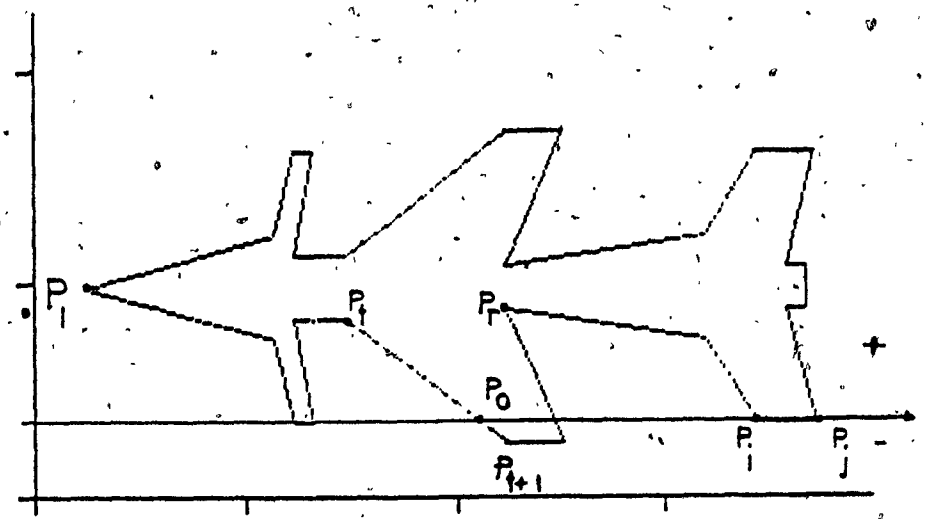

Figure 3.6: Finding the length $\overline{P_tP_o}$ to the left of the current link $\overline{P_iP_j}$, where $t < r$, $|t - r| \neq 1$, (step 4.)

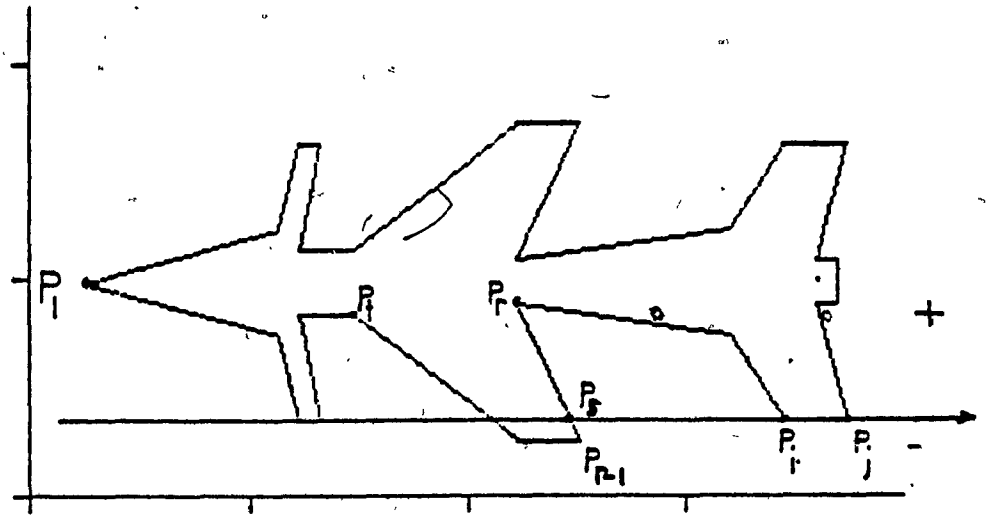

Figure 3.7: Finding the length $\overline{P_rP_s}$ to the left of the current link $\overline{P_iP_j}$, where $t < r$, $|t - r| \neq 1$, (step 4.)

3.4 Changes to algorithm 3

In order to calculate the area to the left of the current link in steps 1 to 4, find the intersection points between the ray containing the current link and the other links of the polygon. Put these points in their topological order with respect to the order of the other vertices. Change step 5 to find the area enclosed by the polygon defined by the vertices found in steps 1 through 4 using eq. 2.1.

Chapter 4

Classification

In this section curve signatures and Fourier descriptors are used to classify totally unconstrained, handwritten numerals on envelopes collected by United States postal service. In [15], similarity measures based on the signature, angular and positional distance are contrasted. The signature is known to be quite insensitive to such distortions as slant and perspective. Moreover it does not degrade considerably under random noise. Nevertheless, the signature proves to be a useful tool for character classification. A recognition experiment was performed on 840 digitized characters which represented numerical digits 0 through 9, in which the learning and testing sequences consisted of 461 and 379 characters respectively. These handwritten characters of 30 different styles represent a small subset of Suen's data base [12]. Samples of characters used in the experiment with their length and area signatures are shown in Figures 4.1, 4.2 and 4.3. The classification module (refer to introduction) consists of k-NN module and signature verification module. In the first module a rough classification was accomplished by using only the FD's as the feature vector while in the second the ambiguous characters were separated using the signature as the feature vector.

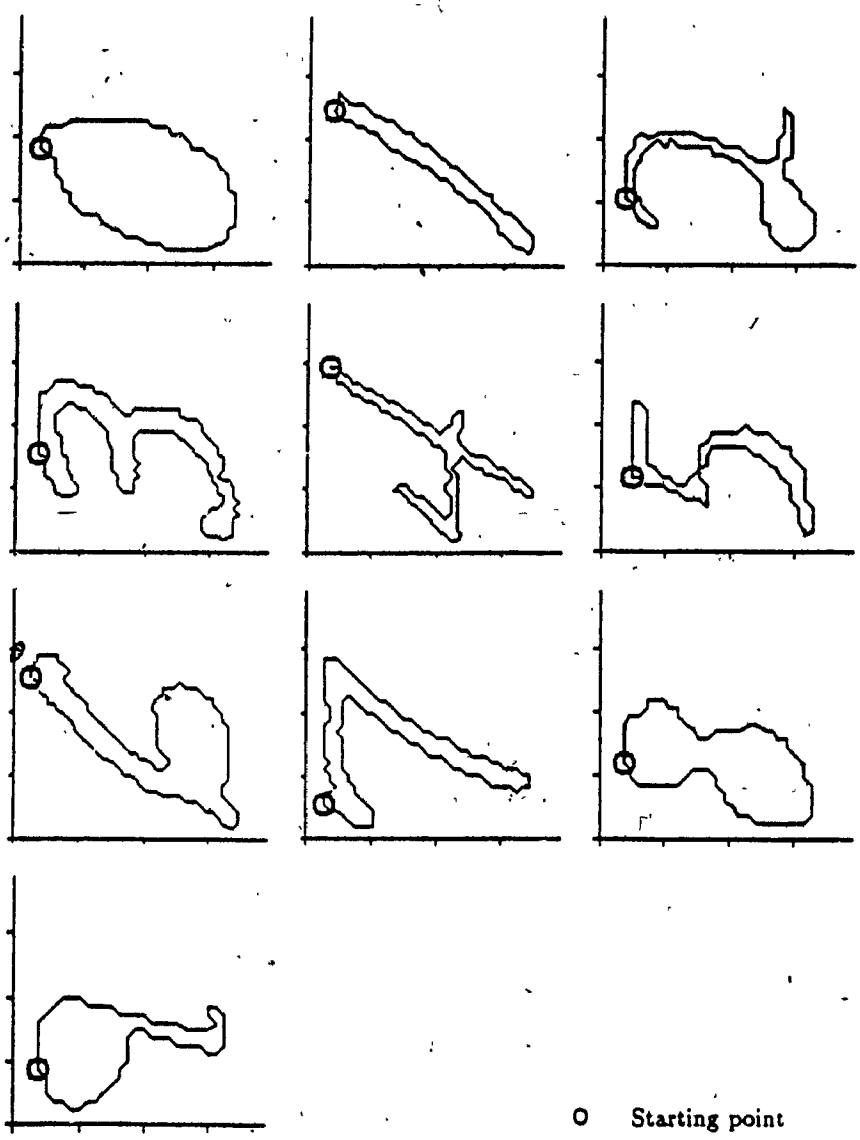

Figure 4.1: Some of the numerals used in the experiment.

The size of the feature vector and the number of the nearest neighbors k which minimized the misclassification rate were experimentally chosen. The optimal k turned out to be 5 (see Table 4.1 and Table 4.2). The effect of mixing the amplitudes A_m and the phase angles α_m in the feature vector were also explored. It was discovered

that the phase angles alone behaved poorly (24% success rate for the length signature and 39% for the area signature (see Table 4.3 and Table 4.4). It was then decided to use only FD's amplitudes as the features in the k-NN module. The optimal number of A_m's amplitudes was 6 for the length signature and 9 for the area signature. With that choice of parameters, an overall recognition rate of 85.5% for both the length and the area signature was achieved (see confusion matrices in Table 4.5 and Table 4.6). These results compare favourably with the literature. Using different FD's Persoon and Fu [17] obtained 84.6% rate and Shridhar and Badreldin [18] 66% rate on a set of carefully selected handwritten characters.

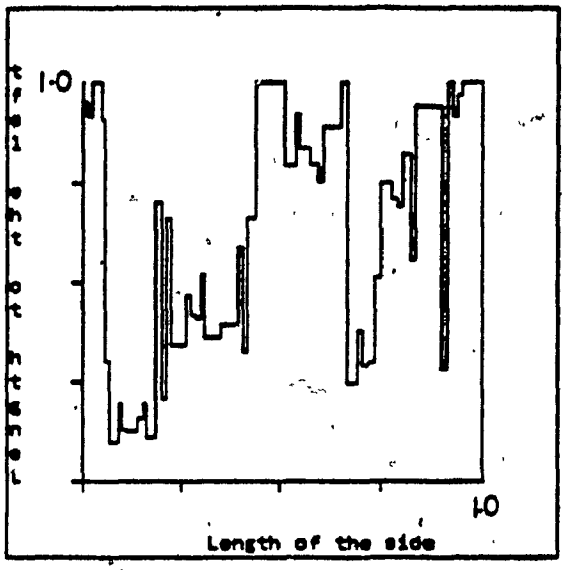

signature of numeral 2.

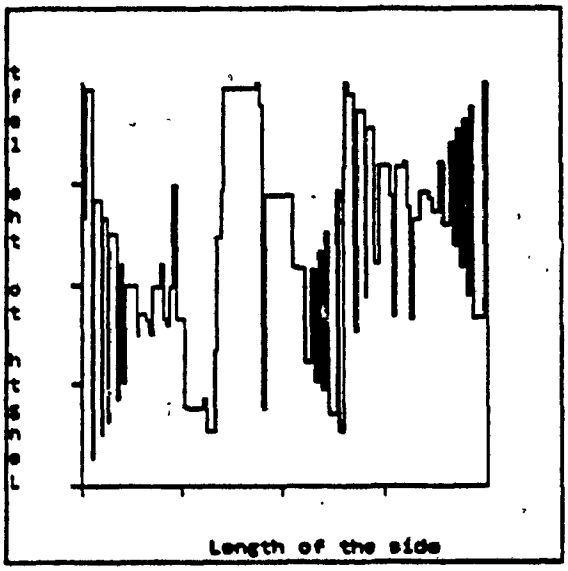

signature of numeral 4.

Figure 4.2: The length signatures of some numerals.

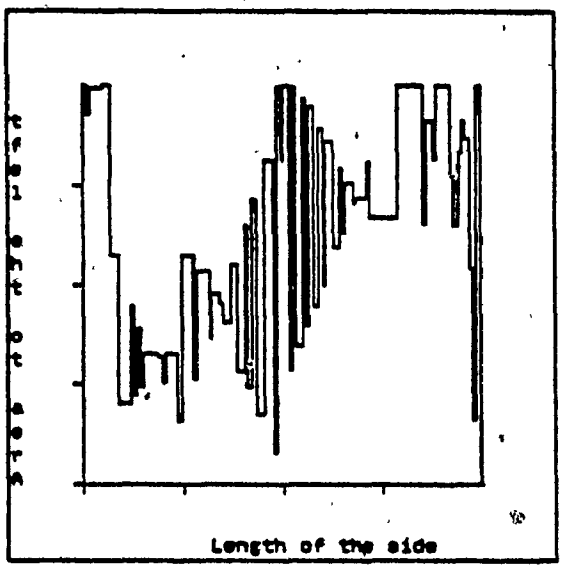

signature of numeral 7.

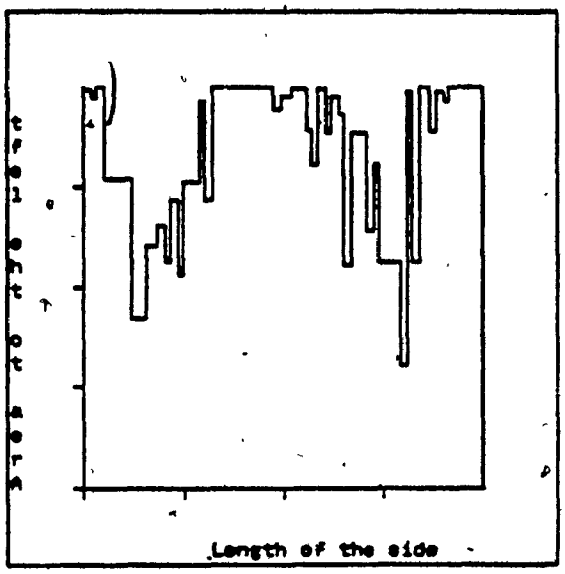

signature of numeral 8.

Figure 4.3: The area signatures of some numerals.

Table 4.1: Classification rates for different sizes of feature vector (FD's (amplitudes) of the length signature) and different number of k-nearest neighbors.

k	number of features (amplitudes)			
	6	9	11	15
4	—	—	—	84.43
5	85.49	85.22	84.43	84.96
7	85.22	74.93	73.61	—
8	—	—	—	80.74
9	79.68	80.21	80.21	80.47
10	78.89	—	—	82.59

Table 4.2: Classification rates for different sizes of feature vector (FD's (phase-angles) of the length signature) and different number of k-nearest neighbors.

k	number of features (phase angles)	
	6	15
5	35.88	24.27
9	24.54	16.89
10	—	17.68

Table 4.3: The confusion matrix for classification using the FD's (phase-angles) of the length signature.

numerals	0	1	2	3	4	5	6	7	8	9	No. of misclassification
0	13	12	3	10	4	4	2	1	2	4	42
1	14	23	1	6	1	4	0	3	1	3	33
2	4	6	10	5	2	1	1	3	3	0	25
3	5	14	3	24	0	1	4	2	0	2	31
4	7	9	4	0	7	0	2	0	0	0	22
5	7	7	1	5	0	2	1	0	2	1	24
6	11	7	4	4	1	0	5	0	1	4	32
7	2	8	1	2	1	0	1	3	0	2	17
8	6	9	4	4	1	0	1	1	1	1	27
9	10	12	2	6	0	3	0	0	1	4	34

The overall results		
	Total	percentage
No. of numeral(s) correctly classified	92	24.27
No. of numeral(s) misclassified	287	75.73

Table 4.4: The confusion matrix for classification using the FD's (phase-angles) of the area signature.

numerals	0	1	2	3	4	5	6	7	8	9	No. of misclassification
0	23	12	5	3	2	0	1	0	4	5	32
1	16	19	5	6	0	1	3	0	5	1	37
2	8	5	15	5	0	0	1	0	0	1	20
3	7	3	2	33	0	0	4	2	3	1	22
4	5	6	7	0	5	0	4	1	0	1	24
5	6	7	0	3	0	1	4	3	1	1	25
6	5	7	0	1	0	1	18	2	1	2	19
7	3	3	4	6	0	0	3	1	0	0	19
8	3	5	7	6	0	1	0	0	3	3	25
9	12	5	3	3	0	2	2	0	0	11	27

The overall results		
	Total	percentage
No. of numeral(s) correctly classified	129	34.04
No. of numeral(s) misclassified	250	65.96

Table 4.5: The confusion matrix for classification using FD's (amplitudes) of the length signature.

numerals	0	1	2	3	4	5	6	7	8	9	No. of misclassification
0	55	0	0	0	0	0	0	0	0	0	0
1	1	53	0	0	0	0	0	0	0	2	3
2	0	0	30	0	0	2	0	0	2	1	5
3	0	0	0	55	0	0	0	0	0	0	0
4	0	4	5	0	17	0	0	2	0	1	12
5	0	0	3	0	0	23	0	0	0	0	3
6	0	0	0	0	0	0	22	0	0	15	15
7	0	0	0	0	2	0	6	12	0	0	8
8	1	3	0	0	0	0	0	0	23	1	5
9	1	0	0	0	0	0	2	0	1	34	4

The overall results		
	Total	percentage
No. of numeral(s) correctly classified	324	85.49
No. of numeral(s) misclassified	55	14.51

Table 4.6: The confusion matrix for classification using FD's (amplitudes) of the area signature.

numerals	0	1	2	3	4	5	6	7	8	9	No. of misclassification
0	55	0	0	0	0	0	0	0	0	0	0
1	0	51	0	0	1	0	0	0	2	1	5
2	0	0	34	0	1	0	0	0	1	0	1
3	0	0	0	55	0	0	0	0	0	0	0
4	0	3	2	1	22	0	0	1	0	0	7
5	0	0	4	0	0	22	0	0	0	0	4
6	0	0	2	0	0	0	17	0	0	18	20
7	0	0	2	0	5	0	2	10	0	1	10
8	2	1	0	0	0	0	0	0	25	0	3
9	0	0	0	0	0	0	4	0	1	33	5

The overall results		
	Total	percentage
No. of numeral(s) correctly classified	324	85.49
No. of numeral(s) misclassified	55	14.51

A glance at the confusion matrices reveals that in many cases 6's were misclassified as 9's, and 4's and 5's as 2's and vice versa, and 6's as 7's. The reason for this phenomenon lies in the rotational invariance of A_m's in eq. (2.3) and mirror reflection invariance of the signature function (so long as the same tracing direction is maintained). Some other numerals are misclassified due to the noise in their outer contour. For example for the length signature:

- 1 is misclassified as 9
- 2 is misclassified as 8
- 2 is misclassified as 9
- 4 is misclassified as 7 and vice versa
- 4 is misclassified as 1 and 9
- 8 is misclassified as 9 and vice versa —see Figure 4.4
- 9 is misclassified as 0

For the area signature:

- 1 is misclassified as 9
- 2 is misclassified as 4 and 8
- 4 is misclassified as 1, 3 and 7
- 6 is misclassified as 2
- 7 is misclassified as 2, 4

- 9 is misclassified as 8

Other numerals which were misclassified because the most important features have almost disappeared are:

- Fat 1 is misclassified as 8
- Fat 1 is misclassified as 0
- Fat 8 is misclassified as 0 —see Figure 4.5
- Thin 8 is misclassified as 1

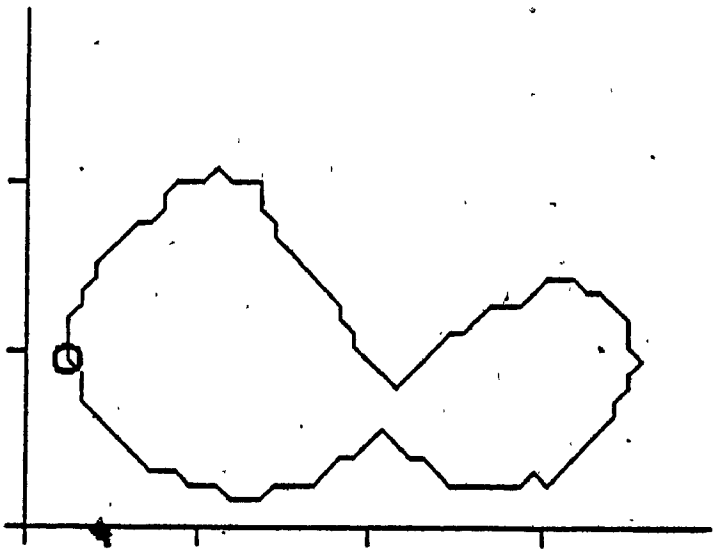

Figure 4.4: Numeral 8 misclassified as 9, because the lower part is small compared to the upper part of the numeral

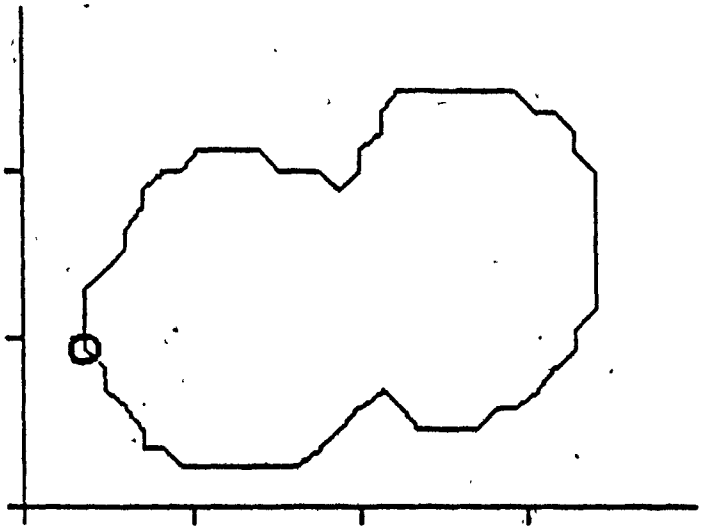

Figure 4.5: Fat numeral 8 misclassified as 0

4.1 Differentiation Scheme

In order to separate the characters which are mirror reflections or rotations of one another a differentiation scheme is used based on the signature itself. The signature is clearly sensitive to reflections and changes in the starting point; therefore, it is used to find the set of discriminating inequalities which are then used to distinguish between easily confused characters. The inequalities in Table 4.7 and Table 4.8 are found experimentally after testing the large set of characters from the learning sequence.

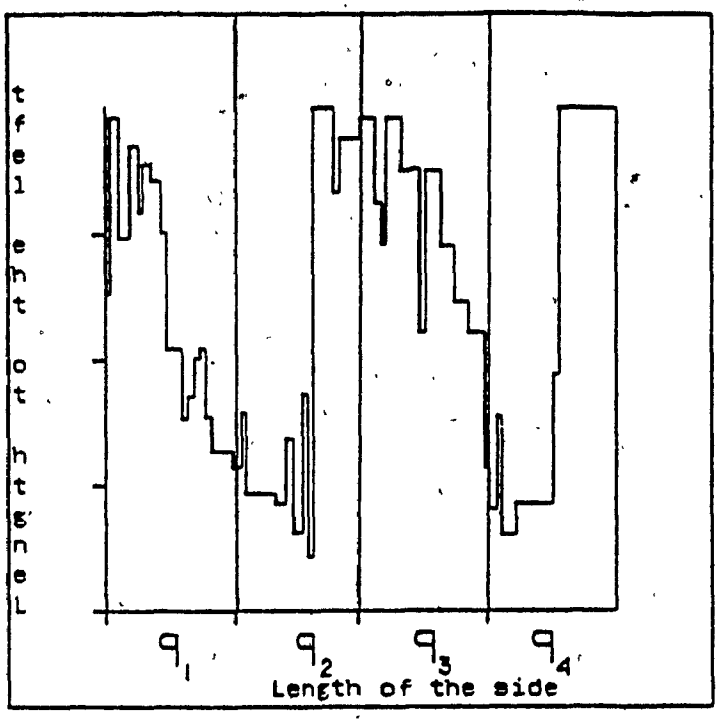

Figure 4.6: The four equal intervals of the signature.

For the length signature the following differentiation scheme is used.

1. For each character, divide the domain of the signature (step function) into four equal intervals and calculate the corresponding areas under the signature, $q_1, \ldots, q_4$, see Figure 4.6.

2. For each category count the number of times $q_i < q_j$, where $1 \leq i, j \leq 4, i < j$.

3. Choose the best 3 inequalities with the highest count number (Table 4.7) to be the template for the category.

4. Assign the character to a class with the maximum number that can satisfy the inequalities in Table 4.7.

Table 4.7: The differentiating inequalities for the length signature.

character	inequalities		
2	$q_1 < q_3$	$q_1 < q_4$	$q_2 < q_4$
4	$q_1 < q_2$	$q_1 < q_3$	$q_1 < q_4$
5	$q_1 < q_2$	$q_2 < q_3$	$q_2 < q_4$
6	$q_1 > q_4$	$q_2 > q_3$	$q_2 > q_4$
7	$q_1 < q_4$	$q_2 < q_3$	$q_2 < q_4$
9	$q_2 < q_3$	$q_2 < q_4$	$q_3 < q_4$

Table 4.8: The differentiating inequalities for the area signature.

character	inequalities					
2	$q_1 < q_2$	$q_1 < q_3$	$q_1 < q_4$	$q_2 < q_3$	$q_2 < q_4$	$q_3 < q_4$
4	$q_1 < q_2$	$q_1 < q_3$	$q_1 < q_4$	$q_2 > q_3$	$q_2 > q_4$	$q_3 < q_4$
5	$q_1 > q_2$	$q_1 < q_3$	$q_1 > q_4$	$q_2 < q_3$	$q_2 < q_4$	$q_3 > q_4$
6	$q_1 > q_2$	$q_1 > q_3$	$q_1 > q_4$	$q_2 > q_3$	$q_2 > q_4$	$q_3 > q_4$
7	$q_1 > q_2$	$q_1 < q_3$	$q_1 < q_4$	$q_2 < q_3$	$q_2 < q_4$	$q_3 < q_4$
9	$q_1 > q_2$	$q_1 > q_3$	$q_1 > q_4$	$q_2 < q_3$	$q_2 < q_4$	$q_3 < q_4$

The similar differentiation scheme for the area signature is used except that 6 inequalities are taken instead of 3 and Table 4.8 is used instead of Table 4.7. These inequalities show the relationship between the four quadrant regions of the numeral. Using these inequalities the class of the confused numeral can easily be identified.

The classification procedure is as follows: using FD's as the coordinates of the feature vector the incoming numeral is assigned by the k-NN module to one class of either set μ_1 or set μ_2. If the incoming numeral is assigned to one class of set μ_1, the real identity of the numeral has been reached. If the incoming numeral is assigned to one class of set μ_2, the k-NN module calls the signature verification module to distinguish between the confused numerals. For example: if the incoming numeral is assigned by k-NN module to class 5 (a member of set μ_2), the signature verification module is used to distinguish between 5 and 2 using the differentiation scheme. The classification schemes for the length and the area signatures incorporating the differentiation schemes are shown in Figure 4.7 and Figure 4.8.

The confusion matrices for the length and area signatures using differentiation schemes are presented in Table 4.9 and Table 4.10. The overall recognition rates using these schemes are 91.03% and 93.14% for the length and area signatures respectively. This clearly shows the superiority of the area signature over the length signature.

Table 4.9: The confusion matrix for the classification scheme using the length signature.

numerals	0	1	2	3	4	5	6	7	8	9	No. of misclassification
0	55	0	0	0	0	0	0	0	0	0	0
1	1	53	0	0	1	0	0	0	0	1	3
2	0	0	32	0	1	0	0	0	2	0	3
3	0	0	0	55	0	0	0	0	0	0	0
4	0	4	4	0	18	1	0	2	0	0	11
5	0	0	3	0	0	23	0	0	0	0	3
6	0	0	0	0	0	0	37	0	0	0	0
7	0	0	0	0	2	0	0	14	0	4	6
8	1	3	0	0	0	0	1	0	23	0	5
9	1	0	0	0	0	0	1	0	1	35	3

The overall results		
	Total	percentage
No. of numeral(s) correctly classified	345	91.03
No. of numeral(s) misclassified	34	8.97

Table 4.10: The confusion matrix for the classification scheme using the area signature.

numerals	0	1	2	3	4	5	6	7	8	9	No. of misclassification
0	55	0	0	0	0	0	0	0	0	0	0
1	0	51	0	0	1	0	0	0	2	1	5
2	0	0	34	0	1	0	0	0	1	0	1
3	0	0	0	55	0	0	0	0	0	0	0
4	0	3	2	1	22	0	0	1	0	0	7
5	0	0	1	0	0	25	0	0	0	0	1
6	0	0	0	0	0	2	35	0	0	0	2
7	0	0	2	0	0	0	0	15	0	3	5
8	2	1	0	0	0	0	0	0	25	0	3
9	0	0	0	0	0	0	1	0	1	36	2

The overall results		
	Total	percentage
No. of numeral(s) correctly classified	353	93.14
No. of numeral(s) misclassified	26	6.86

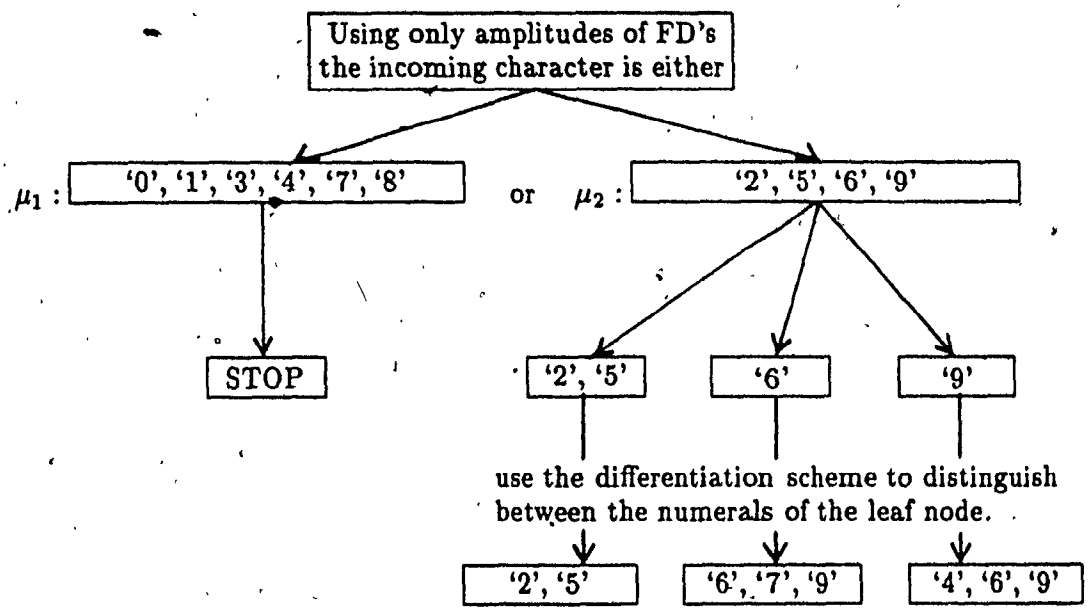

Figure 4.7: The classification scheme for the length signature

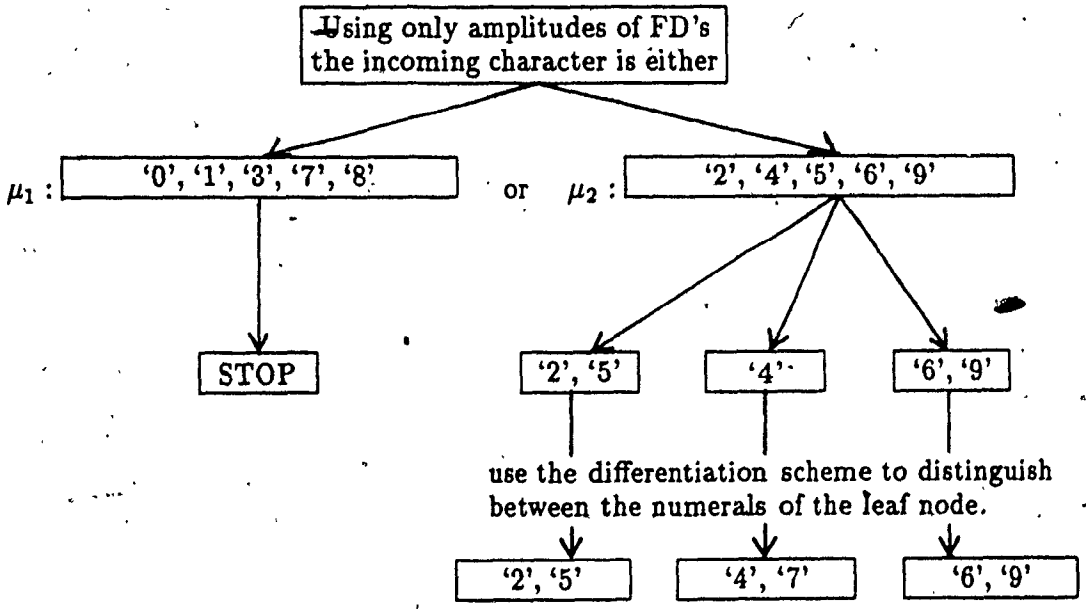

Figure 4.8: The classification scheme for the area signature

Chapter 5

Conclusion

In this project two kinds of curve signatures have been discussed and implemented. Fourier descriptors invariant to affine transformations (translations, rotations and scaling) and changes in starting point have been derived for both signatures. To distinguish between contours which are rotations or mirror reflections of one another the differentiation scheme has been implemented. It has been noted that the area signature performs better than the length signature both with respect to the classification rate and the computational complexity. It is interesting to know how nonlinear distortions affect the signature performance. Another unanswered open question is the fast parallel implementation of the signature computation algorithm.

Bibliography

[1] R. Cosgriff, *Identification of Shape* Technical Report, Ohio State Univ. Res. Foundation, Columbus, December 1960. Rep. 820–11, ASTIA AD 254 742.

[2] F. M. Dekking, and P. J. V. Otterloo, "Fourier Coding and Reconstruction of Complicated Contours," *IEEE Trans. on Syst., Man and Cybern.*, SMC–16(3):395–404, May/June 1986.

[3] S. A. Dudani, and et al. "Aircraft Identification by Moment Invariants," *IEEE Trans. Comput.*, 26:39–46, Jan 1977.

[4] K. Fukunaga, and P. M. Narendra, "A Branch and Bound Algorithm for Computing k–Nearest Neighbor," *IEEE Trans. Comput.*, C–24:750–753, July 1975.

[5] J. E. Goodman, and R. Pollack, "Multidimensional Sorting," *SIAM J. on Computing*, 12:484–507, August 1983.

[6] J. Gorman, O. R. Mitchell, and F. P. Kuhl, "Partial Shape Recognition using Dynamic Programing," *IEEE Trans. on Pattern Anal. and Machine Intell.*, PAMI–10:257–266, March 1988.

[7] H. G. Granlund, "Fourier Preprocessing for Hand Printed Character Recognition," *IEEE Trans. Comput.*, C–21:195–201, Feb 1972.

[8] R. L. Kashyap, and R. Chelappa, "Stochastic Models for Closed Boundary Analysis: Representation and Reconstruction," *IEEE Trans. Inform. Theory*, IT–27:627–637, Sept. 1981.

[9] A. Krzyzak, S. Y. Leung, and C. Y. Suen, "Reconstruction of Two Dimensional Patterns by Modified Fourier Descriptors," 1988. (submitted).

[10] Adam Krzyzak, and Hussein El Buaeshi, "Classification of Digitized Contours Represented by Signature," In *Vision Interface '88*, pages 64–69, Edmonton, Canada, June 1988.

[11] Adam Krzyzak, and Hussein El Buaeshi, "Classification of Digitized Curves Represented by Signatures," In *Third international symposium on handwriting and computer applications*, pages 20–23, Montréal, Canada, July 1987.

[12] M. T. Y. Lai, and C. Y. Suen, "Automatic Recognition of Characters by Fourier Descriptors and Boundary Line Encodings," *Pattern Recognition*, 14(1–6):383–393, 1981.

[13] C. C. Lin, and R. Chelappa, "Classification of Partial 2-D Shapes using Fourier Descriptors," *IEEE Trans. on Pattern Anal. and Machine Intell.*, PAMI–9:686–690, Sept. 1987.

[14] J. O'Rourke, "The Signature of a Plane Curve," *SIAM J. on Computing*, 15:34–51, Feb. 1986.

[15] J. O'Rourke, and R. Washington, "Curve Similarity Via Signature," In *Computational Geometry*, pages 295–317, North–Holland, Netherlands, 1985.

[16] T. Pavlidis, *Structrual Pattern Recognition.* Springer–Verlag, 1977.

[17] E. Persoon, and K. Fu, "Shape Discrimination using Fourier Descriptors," *IEEE Trans. Syst., Man and Cybern.*, SMC–7(3):170–179, March 1977.

[18] M. Shridhar, and A. Badreldin, "High Accuracy Character Recognition Algorithm using Fourier and Topological Descriptors," *Pattern Recognition*, 17(5):515–524, 1984.

[19] C. Y. Suen, M. Berthod, and S. Mori, "Advances in Recognition of Handprinted Characters," *Proceeding of the IEEE*, 68:469–487, April 1980.

[20] C. T. Zahn, and R. Z. Roskies, "Fourier Descriptors for Plane Closed Curves," *IEEE Trans. Comput.*, C–21:269–281, March 1972.

Appendix A

Signature expansion

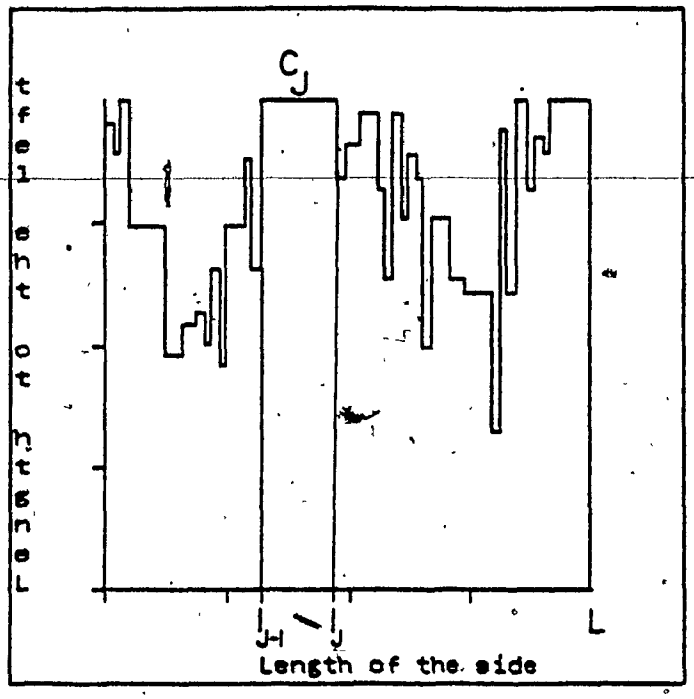

Figure A.1: The signature function.

Where $l_j = l_{j-1} + \Delta l_j$..

The signature $S^*(t) = \sum_{j=1}^{m} c_j \ I_{A_j}(t)$ is a piecewise smooth function on the interval $[0, L]$. In the Fourier series, it can be expanded as follows:

$$\begin{aligned} a_m &= \frac{1}{L}\int_0^L S^*(t)\exp\left(\frac{-i2\pi mt}{L}\right)dt \\ &= \frac{1}{L}\sum_{j=1}^{m} c_j \int_{l_{j-1}}^{l_j} \exp\left(\frac{-i2\pi mt}{L}\right)dt \\ &= \frac{1}{L}\sum_{j=1}^{m} c_j \frac{-L}{i2\pi m}\exp\left(\frac{-i2\pi mt}{L}\right)_{l_{j-1}}^{l_j} \end{aligned}$$

$$= \frac{1}{L}\sum_{j=1}^{m} c_j \frac{iL}{2\pi m}\left\{\exp\left(\frac{-i2\pi m l_j}{L}\right) - \exp\left(\frac{-i2\pi m l_{j-1}}{L}\right)\right\}$$

$$= \frac{1}{2\pi m}\sum_{j=1}^{m} c_j \exp\left(\frac{i\pi}{2}\right)\exp\left(\frac{-i2\pi m l_{j-1}}{L}\right)\left\{\exp\left(\frac{-i2\pi m \Delta l_j}{L}\right) - 1\right\}$$

$$= \frac{1}{2\pi m}\sum_{j=1}^{m} c_j \exp\left(-i\left(\frac{2\pi m l_{j-1}}{L} - \frac{\pi}{2}\right)\right)\left\{\exp\left(\frac{-i2\pi m \Delta l_j}{L}\right) - 1\right\} \quad \text{(A.1)}$$

The real and imaginary parts of a_m are found to be.

$$\exp\left(-i\frac{2\pi m l_{j-1}}{L} - \frac{\pi}{2}\right) = \cos\left(\frac{2\pi m l_{j-1}}{L} - \frac{\pi}{2}\right) - i\sin\left(\frac{2\pi m l_{j-1}}{L} - \frac{\pi}{2}\right)$$

$$\cos\left(\frac{2\pi m l_{j-1}}{L} - \frac{\pi}{2}\right) = \cos\frac{2\pi m l_{j-1}}{L}\cos\frac{\pi}{2} + \sin\frac{2\pi m l_{j-1}}{L}\sin\frac{\pi}{2}$$

$$= \sin\frac{2\pi m l_{j-1}}{L} \quad \text{(A.2)}$$

$$-i\sin\left(\frac{2\pi m l_{j-1}}{L} - \frac{\pi}{2}\right) = -i\left\{\sin\frac{2\pi m l_{j-1}}{L}\cos\frac{\pi}{2} - \sin\frac{\pi}{2}\cos\frac{2\pi m l_{j-1}}{L}\right\}$$

$$= -i\left\{-\cos\frac{2\pi m l_{j-1}}{L}\right\}$$

$$= i\cos\frac{2\pi m l_{j-1}}{L} \quad \text{(A.3)}$$

$$\text{equation A.2} + \text{equation A.3} = \sin\frac{2\pi m l_{j-1}}{L} + i\cos\frac{2\pi m l_{j-1}}{L} \quad \text{(A.4)}$$

$$\exp\left(\frac{-i2\pi m \Delta l_j}{L}\right) = \cos\frac{2\pi m \Delta l_j}{L} - i\sin\frac{2\pi m \Delta l_j}{L} \quad \text{(A.5)}$$

Substituting the equations A.4 and A.5 in the equation A.1 the following is obtained:

$$a_m = \frac{1}{2\pi m}\sum_{j=1}^{m} c_j \left\{\sin\frac{2\pi m l_{j-1}}{L} + i\cos\frac{2\pi m l_{j-1}}{L}\right\}$$
$$\left\{\cos\frac{2\pi m \Delta l_j}{L} - i\sin\frac{2\pi m \Delta l_j}{L} - 1\right\}$$

$$= \frac{1}{2\pi m}\sum_{j=1}^{m} c_j \left\{\sin\frac{2\pi m l_{j-1}}{L}\cos\frac{2\pi m \Delta l_j}{L} - \sin\frac{2\pi m l_{j-1}}{L}\right.$$
$$\left. + \cos\frac{2\pi m l_{j-1}}{L}\sin\frac{2\pi m \Delta l_j}{L} + i\left\{\cos\frac{2\pi m l_{j-1}}{L}\right.\right.$$

$$\cos\frac{2\pi m\Delta l_j}{L} - \sin\frac{2\pi m l_{j-1}}{L}\sin\frac{2\pi m\Delta l_j}{L} - \cos\frac{2\pi m l_{j-1}}{L}\Bigg\}\Bigg\}$$

$$= \frac{1}{2\pi m}\sum_{j=1}^{m} c_j\left\{\sin\left(\frac{2\pi m l_{j-1}}{L} + \frac{2\pi m\Delta l_j}{L}\right) - \sin\frac{2\pi m l_{j-1}}{L}\right.$$
$$\left. + i\left\{\cos\left(\frac{2\pi m l_{j-1}}{L} + \frac{2\pi m\Delta l_j}{L}\right) - \cos\frac{2\pi m l_j}{L}\right\}\right\}$$

$$= \frac{1}{2\pi m}\sum_{j=1}^{m} c_j\left\{\sin\left(\frac{2\pi m}{L}\{l_{j-1} + \Delta l_j\}\right) - \sin\frac{2\pi m l_{j-1}}{L}\right.$$
$$\left. + i\left\{\cos\left(\frac{2\pi m}{L}\{l_{j-1} + \Delta l_j\}\right) - \cos\frac{2\pi m l_{j-1}}{L}\right\}\right\}$$

$$= \frac{1}{2\pi m}\sum_{j=1}^{m} c_j\left\{2\cos\frac{2\pi m}{L}\left(\frac{l_j + l_{j-1}}{2}\right)\sin\frac{2\pi m}{L}\left(\frac{l_j - l_{j-1}}{2}\right)\right.$$
$$\left. + i\left\{-2\sin\frac{2\pi m}{L}\left(\frac{l_j + l_{j-1}}{2}\right)\sin\frac{2\pi m}{L}\left(\frac{l_j - l_{j-1}}{2}\right)\right\}\right\}$$

$$= \frac{1}{2\pi m}\sum_{j=1}^{m} c_j\left\{2\cos\frac{\pi m}{L}(2l_j + \Delta l_j)\sin\frac{\pi m}{L}\Delta l_j\right.$$
$$\left. + i\left\{-2\sin\frac{\pi m}{L}(2l_j + \Delta l_j)\sin\frac{\pi m}{L}\Delta l_j\right\}\right\}$$

$$Re(a_m) = \frac{1}{m\pi}\sum_{j=1}^{m} c_j\cos\frac{\pi m}{L}(2l_{j-1} + \Delta l_j)\sin\frac{\pi m}{L}\Delta l_j \qquad \text{(A.6)}$$

$$Im(a_m) = \frac{-1}{m\pi}\sum_{j=1}^{m} c_j\sin\frac{\pi m}{L}(2l_{j-1} + \Delta l_j)\sin\frac{\pi m}{L}\Delta l_j \qquad \text{(A.7)}$$

Appendix B

Detailed Pseudo-code of algorithm 1

Input: $P_i = (x_i, y_i), 1 \leq i \leq n$.

Output: Signature(i).length/area, $1 \leq i \leq n$.

1. For $i = 1, \ldots, n$ do step 2 to step 9.
2. For $j = 1, \ldots, n$ do $u_j = x_j - x_i$, $v_j = y_j - y_i$.
3. For $j = 1, \ldots, n$, if $(u_j, v_j) \neq (0, 0)$ call j "good".
4. For every good $j = 1, \ldots, n$ let $u_{j+n} = -u_j$, $v_{j+n} = -v_j$, and $s_{j+n} = \frac{v_j}{u_j}$, provided that $u_j \neq 0.0$.
5. The indices $\{j | j$ is good $\} \cup \{n + j | j$ is good$\}$ are to be sorted into subsets as follows
   (a) $\{j | u_j > 0; s_j$ —$key\}$
   (b) $\{j | u_j = 0, v_j > 0\}$
   (c) $\{j | u_j < 0; s_j$ —$key\}$
   (d) $\{j | u_j = 0, v_j > 0\}$.
6. For each $k = 1, \ldots, M$
   - let $N_k[j] = j$ such that $\{\ j \ni j$ is good and each N_k contains the indices of one ray $\}$.
7. Find the vertices to the left of the current link $\overline{P_i P_j}$ as follows: —where $k(j)$ means the number of the subset within which j lies.

- let $g = 0$ and let $k(j) = k_1$; where $N_{k_1}[j] = j$;
- let $k(j+n) = k_2$; where $N_{k_2} = j + n$;
- if $k(j+n) > k(j)$ then
  begin
  - For $e = k(j)+1, \ldots, k(j+n)-1$ do
    begin $g = g + 1$
    For $\mu = 1$ to n do begin if $N_e[\mu] = \mu$ then $\lambda(g) = P_\mu$ end
    end

  end

- if $k(j+n) < k(j)$ then
  begin
  - For $e = k(j)+1$ to M do
    begin $g = g + 1$
    For $\mu = 1$ to n do begin if $N_e[\mu] = \mu$ then $\lambda(g) = P_\mu$ end
    end
  - For $e = 1$ to $k(j+n)-1$ do
    begin $g = g + 1$
    For $\mu = 1$ to n do begin if $N_e[\mu] = \mu$ then $\lambda(g) = P_\mu$ end
    end

  end

8. Sort the vertices in the $\lambda(\cdot)$ array using the index as a key.
9. Signature(i).length = The length of the numeral to the left of the current link. (Compute the length using algorithm 3).
   Signature(i).area = The area bounded by the points on and to the left of the current link. (use eq. 2.1 and algorithm 3).

(In (a) and (c) a list of subsets is obtained; the order within each subset is irrelevant) the result of step 5 is said to be:

$$J_{11}, \ldots, J_{1s_1}, \ldots, J_{M1}, \ldots, J_{Ms_r}.$$

Where the points with indices $J_{k1}, \ldots, J_{ks_1}$ constitute an entire subset and there are M subsets all togther.

Appendix C

Proof of Lemma 2.1

Lemma 2.1. *If Γ and Γ' are two curves which only differ in a sense that they are translation, rotations, or scaled version of each other or they only differ in the starting point by Δl_0 units of arc length then*

$$\begin{aligned} A_m &= A'_m \\ \alpha_m &= \alpha'_m + m\Delta t_0 \end{aligned}$$

Proof: rotation, translation and scaling does not effect the normalized signature $S^*(t)$ so FD's remain the same. Consider the change in the starting point. let $x_0 = U(l)$ and $x'_0 = U'(l)$ be the starting point of Γ and Γ' respectively.

$$U'(l) = U(l + \Delta l_0) \longrightarrow S^{*'}(t) = S^*(t + \Delta t_0)$$

where $\Delta t_0 = \frac{\Delta l_0}{L}$ and $L = 1$. The Fourier coefficients of $S^{*'}(t)$ are

$$\begin{aligned} a'_m &= \int_0^1 S^{*'}(t)\exp(-i2\pi mt)dt \\ &= \frac{1}{2\pi}\int_0^{2\pi} S^{*'}\left(\frac{t}{2\pi}\right)\exp(-imt)dt \\ &= \frac{1}{2\pi}\int_0^{2\pi} S^*\left(\frac{t+\Delta t_0}{2\pi}\right)\exp(-imt)dt \\ &= \exp(im\Delta t_0)\frac{1}{2\pi}\int_0^{2\pi} S^*\left(\frac{t+\Delta t_0}{2\pi}\right)\exp\{-im(t+\Delta t_0)\}d(t+\Delta t_0) \\ &= \exp(im\Delta t_0)a_m \end{aligned}$$

Therefore

$$\begin{aligned} A_m &= A'_m \\ \alpha_m &= \alpha'_m + m\Delta t_0 \end{aligned}$$